

Fluorescent LYVE-1 Antibody to Image Dynamically Lymphatic Trafficking of Cancer Cells *In Vivo*

Michele McElroy, M.D.,* Katsuhiko Hayashi, M.D.,*† Barbara Garmy-Susini, Ph.D.,‡
Sharmeela Kaushal, Ph.D.,* Judith A. Varner, Ph.D.,‡ A. R. Moossa, M.D.,*
Robert M. Hoffman, Ph.D.,*† and Michael Bouvet, M.D.*¹

*Department of Surgery, University of California, San Diego, California; †AntiCancer, Inc., San Diego, California; and ‡Moores Cancer Center, University of California, San Diego, California

Submitted for publication September 28, 2007

Background. The lymphatic system is a major route for cancer cell dissemination, and a potential target for antitumor therapy. Despite ongoing interest in this area of research, the real-time behavior of cancer cells trafficking in the lymphatic system is poorly understood due to lack of appropriate tools to image this process.

Materials and methods. We have used monoclonal antibody and fluorescence technology to color-code lymphatic vessels and the cancer cells inside them in a living animal. Monoclonal anti-mouse LYVE-1 antibody was conjugated to a green fluorophore and delivered to the lymphatic system of a nude mouse, allowing imaging of mouse lymphatics. Tumor cells engineered to express red fluorescent protein were then imaged traveling within the labeled lymphatics in real time.

Results. AlexaFluor-labeled monoclonal anti-mouse LYVE-1 created a durable signal with clear delineation of lymphatic architecture. The duration of fluorescent signal after conjugated LYVE-1 delivery was far superior to that of fluorescein isothiocyanate-dextran or control fluorophore-conjugated IgG. Tumor cells engineered to express red fluorescent protein delivered to the inguinal lymph node enabled real-time tracking of tumor cell movement within the green fluorescent-labeled lymphatic vessels.

Conclusions. This technology offers a powerful tool for the *in vivo* study of real-time trafficking of tumor cells within lymphatic vessels, for the deposition of the tumor cells in lymph nodes, as well as for screening of potential antitumor lymphatic therapies. © 2009 Elsevier Inc. All rights reserved.

Key Words: lymphatics; cancer; mouse models; fluorescence; imaging; real-time; *in vivo*.

¹To whom correspondence and reprint requests should be addressed at 3855 Health Sciences Drive #0987, La Jolla, CA 92093-0987. E-mail: mbouvet@ucsd.edu.

INTRODUCTION

Cancer invasion of the lymphatic system and spread to draining lymph nodes is a common occurrence and is often a first step of the metastatic pathway. Therefore, lymphatic spread is an important component of staging and prognosis [1–3]. Clearly a thorough understanding of the interaction of host lymphatic tissue with invading cancer cells is critical to our ability to fight cancer metastasis.

Current technologies have been able to transiently mark lymphatic architecture [4–6], but no durable strategy for *in vivo* lymphatic visualization has yet been developed. *Ex vivo* immunohistochemical staining of sectioned lymphatic tissue has revealed information on the lymphatic system and its response to specific growth factors, but these are static studies and do not reveal information on the dynamics of cancer cell trafficking within lymphatics [3].

The discovery of lymphatic endothelium-specific markers have allowed the distinction of blood *versus* lymphatic vessels in histological sections, greatly improving our ability to evaluate lymphatic-specific phenomena [7]. We have combined the staining specificity of a monoclonal antibody that binds to murine LYVE-1 located on lymphatic endothelial cells, with the power of *in vivo* fluorescence imaging to facilitate real-time color-coded imaging of lymphatic vessels and tumor cell trafficking in a living animal.

MATERIALS AND METHODS

Antibody Conjugation

Monoclonal anti-mouse LYVE-1 antibody (rat IgG2_a) was purchased from R&D Systems Inc. (Minneapolis, MN). The AlexaFluor 488 monoclonal antibody labeling kit was purchased from Molecular

Probes Inc. (Eugene, OR). The AlexaFluor 488 reactive dye contains a tetrafluorophenyl ester group that reacts with the primary amines of proteins to form stable protein–dye conjugates. Monoclonal anti-mouse LYVE-1 was reconstituted at 1 mg/mL in phosphate-buffered saline (PBS). One hundred microliters of the 1 mg/mL solution was added to the AlexaFluor 488 reactive dye mixture. The pH of the antibody–dye mixture was adjusted to 8.0–8.3 using 1M sodium bicarbonate as needed. The mixture was then allowed to incubate for 1 hour at room temperature, followed by overnight incubation at 4°C. The conjugated antibody was then separated from the remaining unconjugated dye on a purification column by centrifugation. Antibody and dye concentrations in the final sample were determined spectrophotometrically based on absorbance of the final purified conjugate at 280 and 494 nm, respectively.

Control purified rat IgG was purchased from R&D Systems Inc. For conjugation of this antibody, the AlexaFluor 488 protein labeling kit was purchased from Molecular Probes Inc. The control IgG was diluted to 2 mg/mL in PBS. Five hundred microliters of the diluted antibody was added to the AlexaFluor 488 reactive dye mixture. Sodium bicarbonate 1M was used to adjust the pH of the antibody–dye mixture to 8.0–8.3. The mixture was allowed to incubate for 1 hour at room temperature, followed by overnight incubation at 4°C. The conjugated antibody was then separated from the remaining unconjugated dye on an elution column by gravity. Antibody and dye concentrations in the final purified sample were determined spectrophotometrically based on absorbance of the final conjugate at 280 and 494 nm, respectively. All conjugated antibody used in this study had reached a minimum molar ratio of 1:4 mol IgG:mol dye.

Immunohistochemical Staining

Slides of murine axillary lymphatic tissue were fixed using ice-cold acetone for 2 minutes, then stored at -80°C . The slides were then blocked for 12 hour with 5% bovine serum albumin in PBS at 4°C. They were then washed with PBS and incubated with a 1:40 dilution of labeled antibody (0.043 $\mu\text{g}/\text{mL}$ concentration) for 3 hour at room temperature. The slides were then rinsed with PBS and secured with 80% glycerol and a coverslip. Slides were imaged using a

Nikon DE-300 fluorescent inverted microscope (Nikon Instruments, Inc., Melville, NY) and Spot camera RD for image acquisition. Image analysis was done using Metamorph software (Universal Imaging Corporation, Sunnyvale, CA).

Murine mesentery samples from naïve nude mice were spread over glass slides and fixed using acetone at room temperature for 2 minutes and then stored at -80°C . Slides were blocked for 12 hour in 5% bovine serum albumin in PBS at 4°C, washed with PBS, and incubated with 1:100 dilution of labeled antibody (0.02 $\mu\text{g}/\text{mL}$ concentration) for 3 hours at room temperature. Following staining, the slides were rinsed again with PBS and secured with 80% glycerol and a coverslip and then imaged using fluorescence inverted microscopy as above.

Cell Culture

The human pancreatic cancer cell line XPA-1 was a gift from Dr. Anirban Maitra at Johns Hopkins University [8–10]. Cells were maintained in RPMI 1640 media supplemented with 10% fetal bovine serum and 2 mM glutamine from Gibco-BRL, Life Technologies, Inc. (Grand Island, NY). All cells were cultured at 37°C in a 5% CO_2 incubator.

Red Fluorescent Protein (RFP) Retroviral Transduction and Selection

The pDsRed-2 vector from Clontech Laboratories, Inc. (Palo Alto, CA) was used for stable expression of RFP in the human pancreatic cancer cell line XPA-1. The pDsRed-2 retrovirus, which also contains a neomycin-resistance gene, was produced in PT67 packaging cells [11, 12]. Twenty percent confluent XPA-1 cells were incubated with retroviral supernatants of the packaging cells for 24 h. Fresh medium was then replenished and the cells were allowed to grow for another 12 h. This was repeated until high levels of RFP expression were observed under fluorescence microscopy. Cells were then trypsinized and harvested and subcultured in selective media containing Geneticin G418 from Invitrogen Corp. (Carlsbad, CA). The level of G418 was increased in a stepwise fashion from 200 to 2000

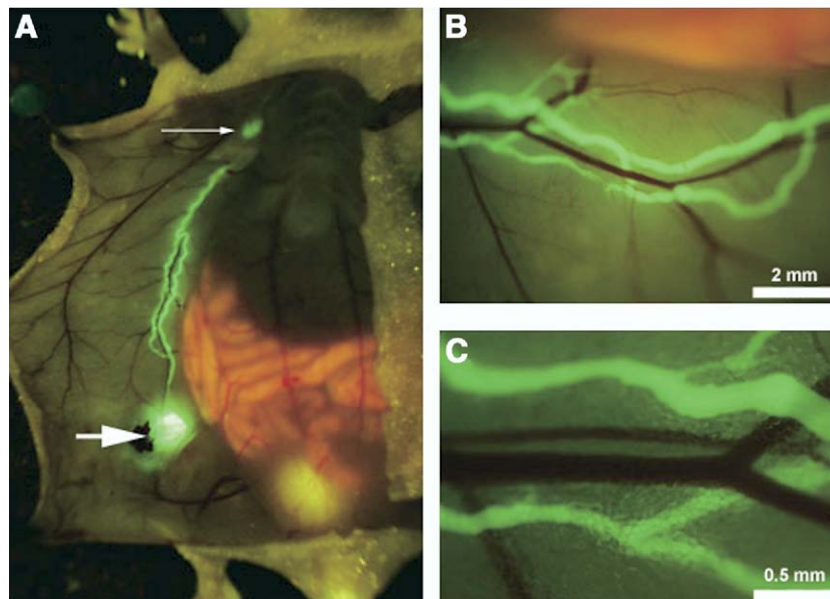


FIG. 1. Fluorescence imaging of *in vivo* murine lymphatic system of the anterior abdominal wall after injection of AlexaFluor-conjugated LYVE-1 to the inguinal lymph node. The inguinal (A, large arrow) and axillary (A, small arrow) lymph nodes, as well as the connecting lymphatics of the anterior abdominal wall (A–C) reveal durable fluorescent staining after delivery of AlexaFluor-conjugated monoclonal anti-mouse LYVE-1 antibody. Neighboring blood vessels did not stain (B, C).

$\mu\text{g}/\text{mL}$. Clones with high RFP expression were isolated and grown for 10 passages in the absence of G418 to select for stable *in vitro* expression of RFP.

In Vivo Lymphatic Imaging with LYVE-1

Six-week-old athymic nude mice were anesthetized using 50% ketamine, 38% xylazine, and 12% acepromazine maleate injected intramuscularly at a dose of $2 \mu\text{L}/\text{g}$. A ventral skin flap was elevated under sterile conditions exposing the inguinal and axillary lymph nodes as well as the interconnecting lymphatics of the anterior abdominal wall. Antibody ($2.4 \mu\text{g}$ conjugated LYVE-1 or control IgG) or fluorescein isothiocyanate (FITC)-dextran (molecular weight, 200,000; Sigma-Aldrich, St. Louis, MO) in a final volume of $50 \mu\text{L}$ was injected slowly into the tissues around the exposed inguinal lymph node using a $50 \mu\text{L}$ Hamilton syringe (Hamilton Co., Reno, NV). For repeated imaging, the skin flap was sutured closed between imaging sessions, again under sterile conditions, using 6-0 polysorb surgical suture (US Surgical, Norwalk, CA).

The inguinal lymph node, draining lymphatics, and axillary lymph node were imaged using the OV-100 Small Animal Imaging System (Olympus Corp., Tokyo, Japan) containing an MT-20 light source from Olympus Biosystems (Planegg, Germany) and DP70 CCD camera from Olympus Corp. Images were processed for contrast and brightness and analyzed with the use of Photoshop Element-4. Animals were imaged immediately after antibody or FITC injection and at 4, 12, 24, 36, 48, and 72 hour post-injection. A total of three mice were used for the *in vivo* time course evaluation. All animal studies were conducted in accordance with the principles and procedures outlined in the NIH Guide for the Care and Use of Animals under Assurance Number A3873-1.

In Vivo Tumor Cell Trafficking

Confluent XPA-1 RFP cells were harvested by trypsinization and washed with warm PBS. The cells were diluted to 10^7 cells/mL in PBS to a total volume of $200 \mu\text{L}$. The cells were slowly and directly injected into the area around the inguinal lymph node using a 1 mL 27G2 latex-free syringe (Becton Dickinson, Franklin Lakes, NJ) 4 hours after administration of AlexaFluor-labeled monoclonal anti-mouse LYVE-1 as described above. Cell movement through the draining lymphatics of the inguinal lymph node and the afferent lymphatics of the axillary lymph node was imaged in real-time using the OV-100 Small Animal Imaging System. Six animals were used in the *in vivo* imaging of tumor cell trafficking over the course of this study.

RESULTS

In vivo lymphatic imaging using AlexaFluor-conjugated LYVE-1 provided a specific and durable signal. Delivery of conjugated LYVE-1 to the mouse inguinal lymph node allowed both immediate and delayed visualization of the draining inguinal lymphatics as well as the afferent lymphatics of the receiving axillary lymph node (Fig. 1A–C). This signal was detectable out to at least 48 hour post-injection with the clearest signal present at 4 hour after antibody delivery. Animals imaged similarly after administration of control conjugated IgG or FITC-dextran to the inguinal lymph node showed minimal signal in the draining lymphatics at 4 hour post-injection and no signal at 12 hour post-injection (Fig. 2). Durable *in vivo* staining of mouse lymphatics was observed in all three animals imaged over time.

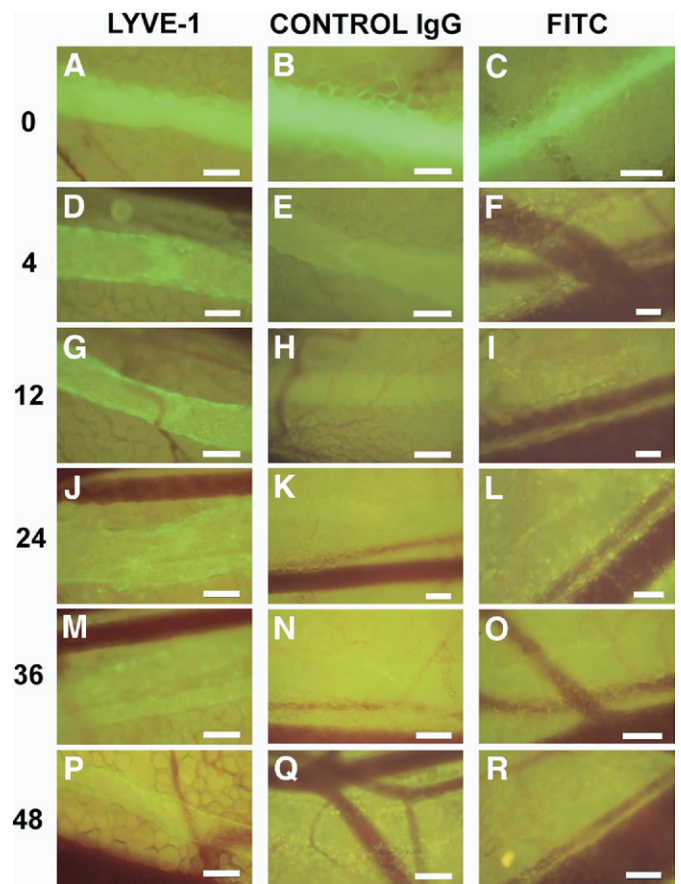


FIG. 2. *In vivo* time course of fluorescence imaging of mouse lymphatics labeled with a one-time dose of fluorescent-labeled anti-LYVE1 antibody *versus* control fluorescent-labeled IgG or FITC-dextran. The hours post-delivery are denoted to the left of the images. All scale bars represent 0.1 mm. While there is comparable fluorescence within the lymphatics immediately after antibody or FITC delivery (A–C), after 4 hours the unbound compound has washed away, leaving a strong positive signal only within the LYVE-1-labeled lymphatics (D–F). The small amount of nonspecific binding present within the conjugated IgG lymphatics at 4 hour post-delivery (E) was completely gone by 12 hours after delivery (H). After a single administration of conjugated anti-LYVE1 antibody, the fluorescent signal remained present for up to 48 hour in the living animal (P). See the Materials and Methods section for antibody-labeling procedures and means of *in vitro* delivery.

Immunostaining of murine lymphatic tissue using AlexaFluor-conjugated LYVE-1 is specific to lymphatic endothelium. Specificity of the conjugated LYVE-1 antibody was verified by *ex vivo* analysis of mouse lymphatic tissue. Murine axillary lymphatic tissue revealed a strong fluorescent signal in the lymphatic vessels around the lymph node periphery with sparing of the germinal centers (Fig. 3A–C). Likewise, staining of prepared mouse mesentery showed specific staining of lymphatic vessels coursing alongside mesenteric arteries and veins with low background (Fig. 3D). In addition, specific *in vivo* binding of the antibody-AlexaFluor conjugate to the endothelium of

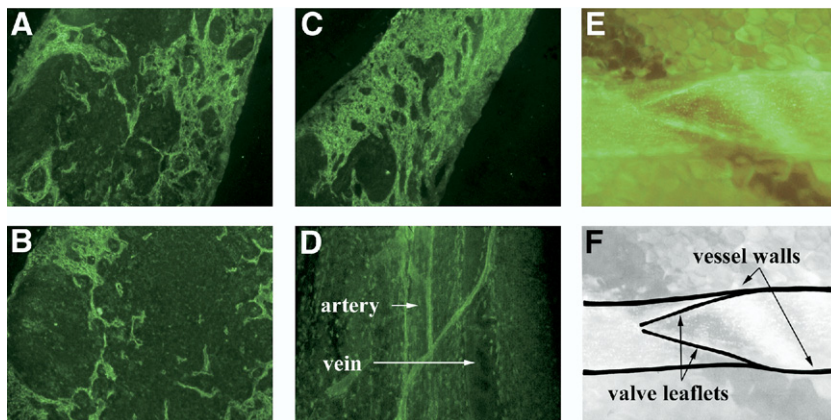


FIG. 3. Fluorescent images of nude mouse axillary lymph node (A–C) and mesentery (D) stained with AlexaFluor-labeled anti-LYVE1 monoclonal antibody. Stained lymphatic tissue was imaged using a fluorescent inverted microscope at $\times 10$ (D), $\times 20$ (C), and $\times 40$ (A, B). Fluorescence microscopy showed staining of lymphatic vessels at the lymph node periphery with sparing of the follicles (A–C). Lymphatic vessels showed positive fluorescence, while neighboring arteries and veins within the tissue did not stain (D). Binding of conjugated LYVE-1 to the lymphatic endothelium *in vivo* outlines vessel walls and valves (E, F).

the lymphatic vessels allowed clear delineation of the vessel walls and valves (Fig. 3E and F).

Tumor cell trafficking through mouse lymphatics imaged with AlexaFluor-conjugated LYVE-1 was imaged *in vivo* in real-time using live-mouse fluorescent imaging technology previously developed in our laboratory [13–15]. After *in vivo* staining of mouse lymphatic endothelium with AlexaFluor-conjugated LYVE-1, human pancreatic tumor cells expressing RFP were injected into the inguinal lymph node and surrounding tissues and lymphatic trafficking was imaged. The RFP-expressing cancer cells were clearly visible within the lymphatic vessels trafficking from the inguinal lymph node to the axillary lymph node (Fig. 4). Fig. 4A–F shows trafficking of RFP cancer cells in a fluorescent LYVE-1-labeled lymphatic. Fig. 4G shows the RFP labeled cancer cells collecting in the receiving axillary lymph node that has also been labeled with the fluorescent LYVE-1 antibody. Cell trafficking through the lymphatic vasculature and into the receiving lymph node can also be imaged and recorded on video in real-time using the Olympus OV-100 Small Ani-

mal Imaging System. In all six animals evaluated for *in vivo* imaging of tumor cell trafficking, the RFP-expressing cancer cells could be reliably seen in contrast against the green-labeled lymphatics.

DISCUSSION

Cancer invasion of the lymphatic system and spread to draining lymph nodes are a common occurrence and are often a first stop of the metastatic pathway [3]. Therefore, lymphatic spread is a significant component of staging and prognosis in many solid tumors [1, 2]. Recent results suggest that lymphangiogenesis itself can contribute to tumor metastasis [16, 17]. In some cases tumor cells appear to influence the host lymphatic architecture, possibly paving the way for their own metastasis [18], although this influence varies with different tumor types [19–21]. These findings underscore the importance of a thorough understanding of the interaction of host lymphatic tissue with invading cancer cells. A clear comprehension of the *in vivo* real-time interactions of tumor cells with their sur-

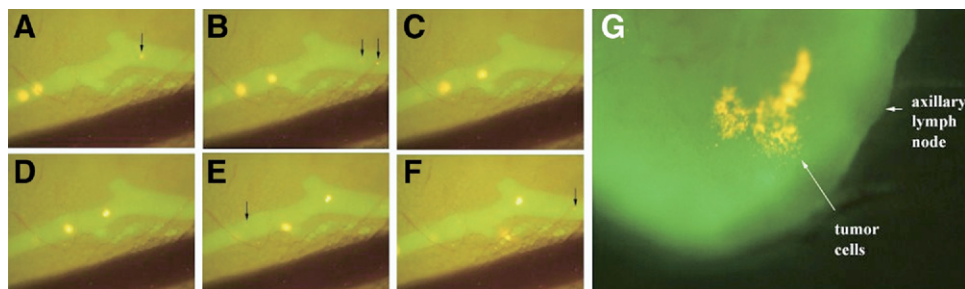


FIG. 4. Sequential images of cancer cells traveling through anterior abdominal wall lymphatics. Following administration of conjugated LYVE-1, the pancreatic cancer cell line XPA-1 RFP was injected into the inguinal lymph node. RFP-labeled XPA-1 cells, both individually (small arrows) and in clusters, could be seen traveling through the fluorescent LYVE-1-labeled lymphatics. (A–F) RFP-labeled cancer cells could also be seen collecting in the axillary lymph node after labeling of the node and lymphatics with green fluorescent LYVE-1 antibody (G).

rounding environment, including the host lymphatic system, would greatly contribute to our ability to understand tumor invasion and metastasis. In particular, imaging of the real-time dynamics of cancer cell trafficking to lymph nodes is critical to the fundamental understanding of metastasis.

Current technologies for lymphatic imaging are often limited to the general uptake of molecules from the interstitial space, affording only transient and nonspecific visualization of the lymphatic system. *Ex vivo* immunohistochemical staining of sectioned lymphatic tissue has revealed information on the lymphatic system and its response to specific growth factors [3]. However, these are static studies and do not reveal information on the dynamics of cancer cell trafficking in lymphatics. Experimental *in vivo* lymphangiography relies on the lymphatic uptake of molecules such as ferritin or FITC-dextran [4–6]. In clinical practice, lymphatic mapping employs the use of radiocolloid solutions or dyes [22, 23]. While these strategies can provide information about lymphatic vessel density and function, they are transient and nonspecific and do not yield information on real-time cancer cell trafficking through lymphatic networks.

LYVE-1 is a hyaluronic acid receptor with sequence similarity to CD44 expressed on lymphatic endothelial cells [24]. This marker as well as other lymph-specific markers such as Podoplanin and vascular endothelial growth factor receptor-3 have made it possible to distinguish between lymphatic and vascular endothelium in *ex vivo* tissue staining, as these markers are generally not expressed on the endothelial cells lining arteries and veins [7]. Monoclonal antibodies specific for LYVE-1 have been used in immunohistochemical staining for some time, but to date have not been used for *in vivo* lymphangiography. We describe here a novel real-time dual-color imaging technology in live mice using fluorescein-conjugated LYVE-1 antibodies to simultaneously visualize lymphatic vessels and lymphatic trafficking of fluorescent-protein-labeled tumor cells traveling within them.

By using monoclonal antibodies specific for the lymphatic endothelium, the technology described in this report enables superior visualization of the anatomy of the lymphatic vessels themselves. Most importantly, the signal remains within the local lymphatic vessels for up to 48 h, conferring ability to image intralymphatic cancer cell trafficking in real-time. Because the antibody-AlexaFluor conjugate can outline the vessel wall rather than merely filling the lumen, we are able to follow cell movement throughout the lymphatic system using tumor cells engineered to express a different colored fluorescent protein, in this case, RFP.

A recent report showed expression of LYVE-1 on a rare subset of tissue macrophages, which may account for some of the LYVE-1-positive cells found in immu-

nohistochemical staining of tumor tissue [25]. Because the uptake of the conjugated antibody relies on functional lymphatics, the likelihood that macrophages contribute significantly to our *in vivo* signal is very low. There has also been a suggestion that LYVE-1 can stain blood vessels in special cases [6]. However, as can be seen in Fig. 1B and C and Fig. 3D, no blood vessels appear to be stained in our model with LYVE-1.

In summary, we have taken advantage of combining lymphatic-specific marker LYVE-1 and fluorescent protein-labeled cancer cells to develop a model system for real-time color-coded imaging of the interaction of tumor cells with the host lymphatic system. Cancer-cell trafficking confirms that the LYVE-1-marked structures in this model system are functional lymphatic vessels. This new technology offers unique advantages over current technologies available for *in vivo* lymphangiography in that lymphatic functionality (tumor-cell trafficking) is imaged in real-time and will facilitate the advancement of our understanding of both interactions of primary tumors with the host lymphatic system as well as lymphatic dissemination of cancer cells. Future studies will also determine clinical use of this powerful imaging technology.

ACKNOWLEDGMENTS

This work was supported by NIH Grant R21 CA109949-01 and American Cancer Society grant RSG-05-037-01-CCE (M.B.) and National Cancer Institute Grants CA099258 and CA103563 (AntiCancer, Inc.). The authors declare that they have no significant competing financial, professional, or personal interests that might have influenced the performance or presentation of the work described in this article.

REFERENCES

1. Rizk N, Venkatraman E, Park B, et al. The prognostic importance of the number of involved lymph nodes in esophageal cancer: Implications for revisions of the American Joint Committee on Cancer staging system. *J Thorac Cardiovasc Surg* 2006;132:1374.
2. Singletary SE, Connolly JL. Breast cancer staging: Working with the Ed. 6 of the AJCC Cancer Staging Manual. *CA Cancer J Clin* 2006;56:37; quiz 50.
3. Stacker SA, Achen MG, Jussila L, et al. Lymphangiogenesis and cancer metastasis. *Nat Rev Cancer* 2002;2:573.
4. Boardman KC, Swartz MA. Interstitial flow as a guide for lymphangiogenesis. *Circ Res* 2003;92:801.
5. Hoshida T, Isaka N, Hagendoorn J, et al. Imaging steps of lymphatic metastasis reveals that vascular endothelial growth factor-C increases metastasis by increasing delivery of cancer cells to lymph nodes: Therapeutic implications. *Cancer Res* 2006;66:8065.
6. Padera TP, Kadambi A, di Tomaso E, et al. Lymphatic metastasis in the absence of functional intratumor lymphatics. *Science* 2002;296:1883.
7. Ji RC. Lymphatic endothelial cells, lymphangiogenesis, and extracellular matrix. *Lymphat Res Biol* 2006;4:83.
8. Berman DM, Karhadkar SS, Hallahan AR, et al. Medulloblastoma growth inhibition by hedgehog pathway blockade. *Science* 2002;297:1559.

9. Berman DM, Karhadkar SS, Maitra A, et al. Widespread requirement for Hedgehog ligand stimulation in growth of digestive tract tumours. *Nature* 2003;425:846.
10. Calhoun ES, Hucl T, Gallmeier E, et al. Identifying allelic loss and homozygous deletions in pancreatic cancer without matched normals using high-density single-nucleotide polymorphism arrays. *Cancer Res* 2006;66:7920.
11. Le Doux JM, Morgan JR, Snow RG, et al. Proteoglycans secreted by packaging cell lines inhibit retrovirus infection. *J Virol* 1996;70:6468.
12. Miller DG, Miller AD. A family of retroviruses that utilize related phosphate transporters for cell entry. *J Virol* 1994;68:8270.
13. Yamauchi K, Yang M, Jiang P, et al. Development of real-time subcellular dynamic multicolor imaging of cancer-cell trafficking in live mice with a variable-magnification whole-mouse imaging system. *Cancer Res* 2006;66:4208.
14. Hoffman RM, Yang M. Color-coded fluorescence imaging of tumor-host interactions. *Nat Prot* 2006;1:928.
15. Hoffman RM. The multiple uses of fluorescent proteins to visualize cancer in vivo. *Nat Rev Cancer* 2005;5:796.
16. Saharinen P, Tammela T, Karkkainen MJ, et al. Lymphatic vasculature: Development, molecular regulation and role in tumor metastasis and inflammation. *Trends Immunol* 2004;25:387.
17. Matsumoto K, Nakayama Y, Inoue Y, et al. Lymphatic microvessel density is an independent prognostic factor in colorectal cancer. *Dis Colon Rectum* 2007;50:308.
18. Qian CN, Berghuis B, Tsarfaty G, et al. Preparing the "soil": the primary tumor induces vasculature reorganization in the sentinel lymph node before the arrival of metastatic cancer cells. *Cancer Res* 2006;66:10365.
19. Rubbia-Brandt L, Terris B, Giostra E, et al. Lymphatic vessel density and vascular endothelial growth factor-C expression correlate with malignant behavior in human pancreatic endocrine tumors. *Clin Cancer Res* 2004;10:6919.
20. Sipos B, Kojima M, Tiemann K, et al. Lymphatic spread of ductal pancreatic adenocarcinoma is independent of lymphangiogenesis. *J Pathol* 2005;207:301.
21. Wong SY, Haack H, Crowley D, et al. Tumor-secreted vascular endothelial growth factor-C is necessary for prostate cancer lymphangiogenesis, but lymphangiogenesis is unnecessary for lymph node metastasis. *Cancer Res* 2005;65:9789.
22. Schoder H, Glass EC, Pecking AP, et al. Molecular targeting of the lymphovascular system for imaging and therapy. *Cancer Metastasis Rev* 2006;25:185.
23. Aarsvold JN, Alazraki NP. Update on detection of sentinel lymph nodes in patients with breast cancer. *Semin Nucl Med* 2005;35:116.
24. Banerji S, Ni J, Wang SX, et al. LYVE-1, a new homologue of the CD44 glycoprotein, is a lymph-specific receptor for hyaluronan. *J Cell Biol* 1999;144:789.
25. Schledzewski K, Falkowski M, Moldenhauer G, et al. Lymphatic endothelium-specific hyaluronan receptor LYVE-1 is expressed by stabilin-1+, F4/80+, CD11b+ macrophages in malignant tumours and wound healing tissue in vivo and in bone marrow cultures in vitro: Implications for the assessment of lymphangiogenesis. *J Pathol* 2006;209:67.